

Impact of fiber fragmentation on mechanical performance and environmental footprint of recycled glass fiber-reinforced polyamide composites

Maja Csapó^{a,b}, József Gábor Kovács^{a,b,*} 

^a Department of Polymer Engineering, Faculty of Mechanical Engineering, Budapest University of Technology and Economics, Műegyetem rkp. 3., H-1111, Budapest, Hungary

^b MTA-BME Lendület Lightweight Polymer Composites Research Group, Műegyetem rkp. 3., H-1111, Budapest, Hungary

ARTICLE INFO

Keywords:

Recycled composites
Glass fiber-reinforced polyamide
Fiber fragmentation
Mechanical properties
Injection molding
Sustainable materials
Carbon footprint

ABSTRACT

Due to their mechanical strength and durability, the automotive industry increasingly incorporates glass fiber-reinforced composites. However, evolving environmental regulations necessitate the integration of recycled materials, presenting challenges, particularly with fiber fragmentation, which compromises composite strength. This study investigates the effects of recycling on the mechanical properties and carbon footprint of polyamide composites reinforced with varying glass fiber contents (15 %, 30 %, 45 %, and 60 %). Injection-molded specimens were subjected to tensile testing to evaluate the effects of varying fiber length distribution on mechanical performance across multiple recycling cycles. Findings revealed that fiber fragmentation increased with successive recycling cycles, decreasing tensile strength and modulus due to shortened fiber lengths. The long fiber ratio of the composites decreased to half after the first recycling. If all fibers were assumed to break below the critical length, strength would drop by 18 %, 28 %, 68 %, and 74 % for PA6-GF15, PA6-GF30, PA6-GF45, and PA6-GF60, respectively, compared to when all fibers stay above the critical threshold. Despite these challenges, the recycled composites retained acceptable structural integrity for specific automotive applications, highlighting their potential market value. Using recycled materials in injection-molded parts can reduce the carbon footprint by up to 30 %, depending on fiber content. Despite increased emissions with higher fiber content, PA6-GF45 offers the optimal balance of strength, modulus, and sustainability. This research provides insight into optimizing fiber content and recycling cycles to balance environmental impact and performance, thereby supporting cleaner production in the automotive sector.

1. Introduction

In recent decades, sustainable development and environmental protection have become crucial worldwide. Lightweight thermoplastic-reinforced composites gradually replace traditional materials with excellent mechanical properties to reduce carbon dioxide emissions by lowering vehicle weight and consequently reducing fuel consumption. One of the economical production methods of thermoplastic composites is fiber injection molding, but this technology generates a large amount of waste. The waste mainly consists of the dropped distribution channel, the recycling of which is a challenge. Thus, considering climate change, global warming, and a sustainable and circular economy, waste management industries have moved towards whole fiber recovery methods

(De. et al., 2024).

In engineering, fibrous structures are the most commonly used reinforcing materials for thermoplastic polymer composites. The mechanical properties of fiber-reinforced composites depend on the fibers' distribution, size and orientation, and the amount of adhesion between the fibers and the matrix. The compatibility between the phases and the grade of fiber dispersion within the matrix also significantly affects the mechanical properties. The most commonly used reinforcing fibers are glass and carbon fibers, but carbon nanotubes, aramid, and basalt fibers are also used (De. et al., 2024). The most commonly used reinforcing fiber is glass fiber due to its low cost and good mechanical properties. The waste reduction of fiber-reinforced thermoplastic composites has received much attention in recent decades, and one solution is recycling.

* Corresponding author. Department of Polymer Engineering, Faculty of Mechanical Engineering, Budapest University of Technology and Economics, Műegyetem rkp. 3., H-1111, Budapest, Hungary.

E-mail addresses: csapom@pt.bme.hu (M. Csapó), kovacs@pt.bme.hu (J.G. Kovács).

<https://doi.org/10.1016/j.jclepro.2025.145678>

Received 8 November 2024; Received in revised form 21 March 2025; Accepted 8 May 2025

Available online 8 May 2025

0959-6526/© 2025 The Authors. Published by Elsevier Ltd. This is an open access article under the CC BY-NC-ND license (<http://creativecommons.org/licenses/by-nc-nd/4.0/>).

In the automotive industry, one of the most commonly used engineering composites is glass fiber–reinforced polyamide; several studies focus on its recycling and the properties of fiber length (Tamrakar et al., 2023; Gonçalves et al., 2022; Pietroluongo et al., 2020; Gopalraj and Karki, 2020; Karimi et al., 2023). Gonçalves et al. (2022) wrote about the effects of mechanical recycling and investigated thermal and chemical recycling, making reclaiming good-quality fibers possible. Fiber recycling is indispensable for fiber-reinforced composites, but their energy requirements have not yet been determined. Therefore, we used mechanical recycling as well. Pietroluongo et al. (2020) also investigated the effects of mechanical recycling on a glass fiber–reinforced PA66 automotive component, comparing microstructural and rheological behavior with mechanical properties. They found that mechanical strength also decreased with recycling due to fiber breakage. However, in spite of degradation, the material retained its mechanical characteristics, which are acceptable for other automotive applications. Thus, mechanical recycling can be a solution to the problem of disposal in landfills. Gopalraj et al. (Gopalraj and Karki, 2020) reached a similar conclusion in their study about the methods of recycling composite waste containing carbon and glass fibers and the recovery of the fibers.

Not only recycling but also intensive processing can damage glass fibers, which affects the mechanical properties of the composite. One of the most common processing methods for thermoplastic fiber-reinforced composites is injection molding. Fibers are subjected to great stresses throughout the injection molding process, including hydrodynamic effects, fiber-to-fiber interactions, and fiber-to-device wall interactions, which can reduce average fiber length (Karimi et al., 2023). One of the main challenges of the injection molding of granules with fibers is the relative orientation of the fibers in the part, which is affected by the high shear rates and long flow paths during mold filling (Kugler et al., 2020). Ensuring that the fibers are highly oriented with the expected loads is challenging, but fiber breakage is also a problem during injection molding, resulting from high shear stresses. A significant shortening of the fibers impairs the mechanical properties of the part (Miscík et al., 2024). Therefore, when the effect of recycling is examined, it is essential to compare the effects of the processing parameters on the mechanical properties of the fibers. Eriksson et al. (1996) investigated the mechanical properties and performance of a recycled PA6.6–30 w% glass fiber composite. The results showed that recycling decreased tensile strength, which the shortening of the fibers can fully explain. This phenomenon was also investigated by Bernasconi et al. (2007) on injection-molded PA 66 GF 35 samples with different grinding ratios. Kuram et al. (2013) studied the effect of the number of processing cycles and injection molding parameters on the mechanical properties of recycled PA6-GF30 samples. The number of recycling cycles had the most significant effect, which they proved with variance analysis. They found that fiber breakage was considerable each time the material was recycled. Güllü Abdulkadir et al. (Güllü et al., 2006) examined the effect of glass fibers on the mechanical properties of PP and PA6. They also examined the effect of fiber content and injection molding parameters on fiber breakage. The experiments showed that fiber reinforcement improved strength, but the improvement did not show a linear relationship with fiber mass fraction. They concluded that fiber breakage is reduced with low screw speed and injection speed, and large gate size.

Rohde et al. (Rohde, 2015) comprehensively investigated the effect of processing parameters on fiber length in the injection molding of long fiber–reinforced thermoplastic polymer parts. They used a design of experiments in which they varied injection rate, back pressure, holding pressure, and screw speed. Their statistical analysis showed that only the combination of increased back pressure and screw speed was significant. However, they found it difficult to isolate the mechanisms that cause fiber breakage due to the complex phase transitions and shearing processes involved in injection molding. Most fiber breakage occurs in the plastification stage, which various research groups along the different zones of the screw investigated. (Turkovich and Erwin, 1983; Inoue et al., 2015; Lafranche et al., 2005). Using a conventional injection

molding machine, Turkovich and Erwin (1983) determined by examining the sections of the screw that most fiber breakage occurs in the compression zone as a result of the high shear because, during plastification, the fibers protruding from the solid bed bend and break off. Inoue et al. (2015) and Lafranche and Krawczak (Lafranche et al., 2005) also found this and showed that the part's quality depends on the gate type and the plastification unit's design. They found that most fiber shortening occurred in the cavity of the plastification unit (nozzle, gate).

There are various methods for measuring fiber shortening during processing and recycling. Among these, the most widespread are optical methods, which measure fiber length and study the relationship between the processing conditions and the fiber length and the mechanical properties of the injection molded parts (Giusti et al., 2018; Kang et al., 2021, 2024). ISO 23314:2006 describes the standardized fiber length measurement for materials with short fiber reinforcement. Generally, the proper measurement of fiber length requires measuring the length of 1000–2000 fibers. Eriksson et al. (1996) used fiber length distribution, average fiber length, and weighted average according to fiber length to characterize recycled 30 m% glass fiber–reinforced PA6.6 samples. Average fiber length can be calculated with Eq. (1); average fiber length indicates the damage of the fibers during processing. Weighted average fiber length can be calculated with Eq. (2):

$$L_N = \frac{\sum_{i=1}^n N_i l_i}{\sum_{i=1}^n N_i} \quad (1)$$

$$L_W = \frac{\sum_{i=1}^n N_i l_i^2}{\sum_{i=1}^n N_i l_i} \quad (2)$$

The whole sample can be represented with a histogram containing n classes, where each class contains N_i fibers of length l_i . The weighted average fiber length (by weight or fiber length) is the characteristic mean of the fiber length distribution (FLD), which emphasizes the proportion of long fibers in the distribution. The number average and weighted average fiber length are commonly used to describe the fiber length distribution (Bernasconi et al., 2007; Bernasconi et al., 2007; Salaberger et al., 2011). In a further study, Bernasconi et al. (Bernasconi et al., 2007) investigated the fatigue behavior of reprocessed glass fiber-reinforced PA6.6. The fiber length distribution was corrected for a more appropriate calculation. A Weibull probability distribution function can describe the FLD, as studies showed that Weibull's model could accurately describe the statistical distributions of the mechanical properties (Breuer et al., 2021; Ding et al., 2024):

$$f(l|s, f) = \frac{f}{s} \left(\frac{l}{s}\right)^{f-1} e^{-(l/s)^f} \quad (3)$$

where l is fiber length, s is the scale factor, and f is the shape factor. On the other hand the cumulative distribution function of the Weibull distribution, Eq. (4) can express the percentage of a measured fiber, which is useful to describe the fibers below and above the critical fiber length:

$$p = F(l|s, f) = \int_0^l f \cdot s^{-f} \cdot \lambda^{f-1} \cdot e^{-\left(\frac{\lambda}{s}\right)^f} d\lambda = 1 - e^{-\left(\frac{l}{s}\right)^f} \quad (4)$$

where p is the probability that a single observation from a Weibull distribution with parameters s and f falls in the interval $[0, l]$. Since the fibers are not of uniform length, repeated injection molding led to a progressively narrower length distribution (Eriksson et al., 1996). Studies showed that with full reprocessing, mean fiber length decreased exponentially to an asymptotic value as the number of reprocessings increased. This asymptotic limit was near critical fiber length, according to Filbert (Curtis et al., 1978). Average fiber length after the n th injection molding cycle if new material is mixed with recycled material (De et al., 2024):

$$L(n) = aR \exp(-n\alpha) + a(1 - R)\exp(-\alpha) + c, \quad (5)$$

where $L(n)$ is the average fiber length after the n th injection molding cycle, R is the ratio of recycled material, c is the asymptotic limit value, and a and α are parameters depending on injection molding parameters. $L(0) = a + b$ is the initial fiber length. When 100 % recycled material is used, $R = 1$:

$$L(n) = a \exp(-n\alpha) + c \quad (6)$$

Studies have shown (Kugler et al., 2020; Miskic et al., 2024; Eriksson et al., 1996; Bernasconi et al., 2007) that the tensile properties of short glass fiber-reinforced thermoplastics primarily result from a combination of matrix and fiber properties, fiber length distribution, and fiber orientation distribution. Bernasconi et al. (2007) determined fiber length distribution by measuring fibers taken from the samples. The fibers were spread on a glass slide and photographed with an optical microscope using a digital camera connected to a computer. The recordings were processed using the image analysis software of the Matlab Image Analysis package. They also used manual measurement to evaluate the fiber length, during which they measured and statistically analyzed 1000 fibers per material. In order to increase the accuracy of the statistics, they corrected fiber length distribution by taking into account the fibers intersecting the image boundaries (Bernasconi et al., 2007). As a result of this correction, the number of relatively long fibers increased, changing the frequency distribution and causing a lower frequency of short fibers. Salaberger et al. (2011) used sub- μm computed tomography (CT) to determine the fiber orientation and fiber length distribution. They applied two analysis concepts on four different fiber content for long glass fiber-filled polypropylene for data evaluation. The parameters of fiber orientation, fiber length distribution, and fiber content have been investigated. The FLD derived from the CT data analysis was systematically compared with the FLD obtained from standard optical microscopy analysis. In a similar study, Cai et al. (2023) investigated the failure mechanisms and the critical fiber length of short glass fiber-reinforced composites, with a focus on the role of micro-structural features such as fiber orientation, fiber-matrix interaction, and pore defects. According to the study, the tensile strength of a composite can be determined by considering the distribution of fibers relative to the critical fiber length Eq. (6).

$$\sigma_c = \eta_0 V_f \bar{\sigma}_f + \bar{\sigma}_m (1 - V_f - V_p) \quad (7)$$

where η_0 is a fiber orientation factor, $\bar{\sigma}_m$ is the average strength of the matrix, V_f is the fiber volume fraction, and V_p is the volume fraction of pores. The average tensile strength $\bar{\sigma}_f$ of a short fiber can be calculated based on a modified Kelly-Tyson model, taking into account both the sub-critical fiber Eq. (7) and the super-critical Eq. (8) fiber contribution (Cai et al., 2023):

$$\bar{\sigma}_f(l < l_c) = \frac{\tau l}{D} + \sigma_0 \quad (8)$$

$$\bar{\sigma}_f(l > l_c) = \sigma_{\max} \cdot \left[1 - \frac{\sigma_{\max} - \sigma_0}{\sigma_{\max}} \cdot \frac{l_c}{2l} \right] \quad (9)$$

where τ_s is the shear strength of the interface and σ_{\max} is the maximum tensile strength of the fiber, which can be defined with the fiber elastic modulus E_f and the maximum strain of the fiber ϵ_f . Due to the introduction of pores in the tensile strength of a short glass fiber-reinforced composite, the prediction of the critical fiber length is more accurate in evaluating glass fiber breakage. Vas (2006) developed formulas to estimate the strength of short fiber-reinforced composites as a function of fiber length and fiber content. In this model a critical adhesion length (l_s) can be defined during a fracture, the resistance of which against pulling out is equal to the breaking load of the fiber:

$$F_s = l_s f_b \quad (10)$$

where f_b is the specific resistance per unit fiber length, and $2l_s$ is called

critical fiber length. If we take the fibers that intersects the breaking cross section, a distribution function of the active beard length (l^+) can be characterized obtained from distribution $Q_l(x) = P(l < x)$, on the basis of the theory of fiber flow (Vas, 2006):

$$S(x) = P(l^+ < x) = \int_0^x \frac{1 - Q_l(t)}{\bar{l}} dt \quad (11)$$

where $\bar{l} = E(l)$ is the expected value of the average fiber length l . For a given fiber, an active beard length l_m can be applied. If $l_m < l_s$ the fiber intersecting the breaking cross section slips out, and in the opposite case, when $l_m > l_s$ the fiber breaks:

$$l_m = \min(l^+, l^-) \quad (12)$$

A distribution function $S_m(x)$ of length l_m can be obtained from beard-length distribution by Eq. (13):

$$S_m(x) = P(l_m < x) = \int_0^{2x} \frac{1 - Q_l(t)}{\bar{l}} dt \quad (13)$$

The relationship between the average tensile strength of the reinforcing structure and the average fiber length, in the presence of simultaneous damage, can be calculated as follows (Vas, 2006):

$$\bar{F}l = f_b \int_0^{l_s} x dS_m(x) + F_s (1 - S_m(l_s)) \quad (14)$$

This relationship enables the effective determination of the tensile strength of a short fiber-reinforced composite, accounting for fiber fragmentation due to fiber content, as well as the presence of fibers both above and below the critical fiber length. Injection molding is crucial in manufacturing due to its versatility and precision in producing complex components. (Moussaoui, 2024). However, the environmental footprint of injection molding has become a significant concern, driven by the energy-intensive nature of the process and the increased use of fossil fuel-based polymers (Nguyen et al., 2024). Addressing the sustainability of injection molding involves understanding the energy consumption and the potential to reduce carbon emissions through optimizations and material recycling (Dollischek et al., 2024).

Life cycle assessment (LCA) methodologies have been extensively applied to evaluate the environmental impacts of various manufacturing processes, including injection molding. However, limitations in current LCA models—particularly in capturing the variability of energy use across different machines and conditions—underscore the need for more refined analyses. For instance, existing LCI databases often use averaged data that does not account for specific factors like machine type, polymer properties, or operational parameters, which can significantly impact energy consumption. A more nuanced approach is necessary for an accurate environmental assessment of injection molding (Nguyen et al., 2024).

Moreover, recent studies highlight the benefits and challenges of incorporating recycled materials in injection molding. By reintroducing materials into production cycles, such as recycled glass fiber-reinforced polyphenylene sulfide (PPS GF40), the demand for virgin resources can be reduced, potentially lowering the carbon footprint (Dollischek et al., 2024). However, recycled materials often exhibit altered mechanical and rheological properties, which must be carefully managed to maintain product quality. The development of allocation methods for environmental impacts, such as the Circular Footprint Formula, provides frameworks for quantifying the benefits of using recyclates in open-loop systems, though further research is needed to standardize these practices for injection-molded products (Tinz et al., 2023).

Optimizing the injection molding process for sustainability requires refining parameters like cycle time and specific energy consumption. Design of experiments (DOE) studies have shown that process parameters significantly impact energy efficiency, with optimized settings capable of reducing both energy use and carbon emissions. This dual focus on process optimization and material selection reflects a broader

trend in the industry toward cleaner production methods (Moussaoui, 2024).

We aim to establish a connection between recycling and material usage by optimizing fiber content and recycling cycles to balance environmental impact and mechanical performance, thereby supporting cleaner production in the automotive industry. This study provides a novel contribution by systematically analyzing the impact of recycling cycles on fiber length distribution and its correlation with the mechanical integrity of polyamide composites. By investigating fiber length fragmentation and its relationship with mechanical performance and carbon footprint, we aim to understand how material properties change during recycling. The research is designed to evaluate fiber length distributions through optical microscopy and assess mechanical properties such as tensile strength, elasticity, and flexural performance, offering insights to guide sustainable composite design.

2. Materials and methods

2.1. Materials

Tarnamid T27 PA6 (Grupa Azoty S.A., Tarnów, Poland) was chosen for this study due to its availability with different glass fiber contents (15 %, 30 %, 45 %, and 60 %), enabling a comprehensive analysis of fiber length distribution and mechanical performance (see Table 1). This material is widely used in automotive applications, making it a relevant candidate for industrial recycling studies. The glass fibers are pre-sized with a coupling agent to enhance adhesion with the polyamide matrix, improving mechanical properties and durability. Since fiber sizing affects fiber behavior during recycling, its influence was also considered when evaluating the effects of multiple recycling cycles on composite performance. The material was dried in a Faithful WGLL-125 BE (Faithful Technology, Cangzhou, China) drying oven at 80 °C for 4 h. Altogether, 5 kg of material was dried for each fiber content.

Table 1
Manufacturer-provided data for material characteristics and processing (before recycling).

Tarnamid T-27	neat	GF15	GF30	GF45	GF60
Manufacturing					
Melt temperature (°C)	240–260	240–280	240–290	240–280	260–280
Mold temperature (°C)	60–80	80–100	60–100	80–100	80–100
Melt volume-flow rate (MVR) 275 °C/5 kg (cm ³ /10 min)	120	60	45	20	n.a.
Injection rate (cm ³ /s)	high	medium	medium	medium	medium
Injection pressure (MPa)	80–110	80–110	60–110	80–110	80–110
Drying (°C)	80 °C/4 h				
Carbon Footprint (CF)					
Average CF (kg CO ₂ /kg PA6)	3.5	4	4.5	5	5.5
Average CF of injection molded part (kg CO ₂ /kg PA6)	5.75	6.25	6.75	7.25	7.75
Average nominal CF per unit of strength per kg of material (g CO ₂ /kg PA6/MPa)	43	31	26	24	23
Average nominal CF per unit of modulus per kg of material (g CO ₂ /kg PA6/MPa)	1.13	0.70	0.47	0.34	0.28

The fiber content was checked with a burn-out test, for which the matrix material was burned out in the Denkal 6B (Kalória Hőtechnikai Kft., Budapest, Hungary) annealing furnace at 550 °C for 3 h. The fiber contents of 12.4 m%, 29.7 m%, 44.2 m%, and 59.8 m% refer to mass percent (m%), representing the proportion of glass fibers relative to the total mass of the composite. The fiber content was determined using the burn-out method according to the ISO 3451-1 and 3451-4 standards, where the polymer matrix is removed through controlled heating, and the remaining fiber mass is measured.

2.2. Methods

We analyzed injection molded specimens to demonstrate the effect of glass fiber length and characterize the effect of recycling on mechanical properties. In the first step, specimens were manufactured from the dried glass fiber-reinforced polyamide granulate on an Arburg 270S 400 170 (ARBURG GmbH, Lossburg, Germany) injection molding machine in a two-cavity mold.

The processing parameters were set based on the material supplier's recommendations to ensure optimal conditions for Tarnamid T27 PA6. The melt temperature was 280 °C. We used a commonly accepted method for the barrel zone temperature settings (280 °C for the nozzle, 280 °C for the following zone, and 270 °C, 260 °C for the following two zones, while the last was set to 250 °C). This temperature profile was selected to ensure complete melting of the polymer while minimizing thermal degradation. The mold temperature was set to constant 80 °C for both mold halves. In addition, the injection rate was 45 cm³/s, following the ISO 1874-2 standard, which specifies processing parameters for polyamide materials to ensure uniform molding conditions and reproducibility.

We used a 30 mm diameter screw with a peripheral speed of 20 m/min and a back pressure of 40 bar. The dimensions of the test specimens were 80 mm × 80 mm × 1.2 mm. Due to the placement of the gates, the specimens contained a weld line (Fig. 2). Subsequently, the remaining specimens at the end of each cycle were granulated using an SB Plastics Machinery grinder, and the 100 % granulated glass fiber-reinforced polyamide material was injection molded for five cycles under the same conditions (Fig. 1).

Our goal is to examine the change in mechanical properties as a function of the number of recycling cycles and, thus, the shortening of fiber length. We characterized fiber shortening by measuring fiber length. We measured it with an optical microscope and then plotted it in a distribution function. We performed tensile tests to test and predict tensile strength, the modulus of elasticity, and flexural strength and modulus.

2.2.1. Microscopic examinations

For the microscopic examination of the glass fibers, we produced samples by burning out the matrix at 550 °C for 3 h. The weight of the samples was measured with a RADWAG PS200/200.RI (RADWAG Balances and Scales, Radom, Poland) scale (accuracy 0.001 g) in ceramic

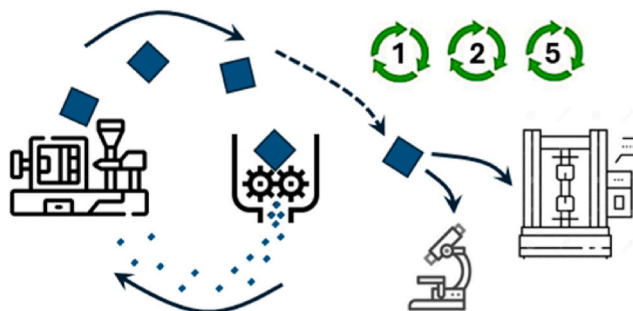


Fig. 1. Injection molding cycles (1, 2, and 5 loops) and mechanical testing of PA6 reinforced with 15 m%, 30 m%, 45 m%, and 60 m% glass fiber.

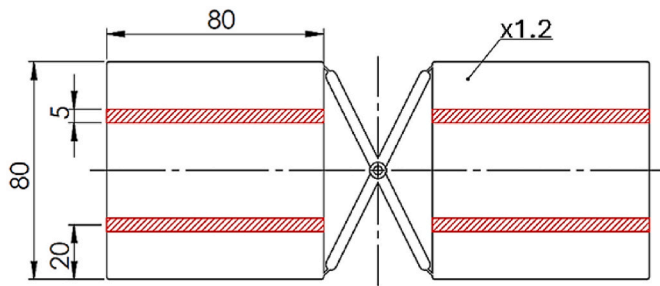


Fig. 2. The part produced with the Arburg 270S 400-170 injection molding machine and the specimens that were cut out, marked with the red area (The center of the mold contains the sprue, while the 'X' in the center of the two parts indicates the runner system. The specimens, measuring 80 mm by 80 mm, are filled through two gates located at the corners. The vertical dashed line shows the position of the resulting weld line.). (For interpretation of the references to colour in this figure legend, the reader is referred to the Web version of this article.)

cups. The samples were burned out in a Denkal 6B (Kalória Hőtechnikai Kft., Budapest, Hungary) annealing furnace. The length of the fibers was measured with a Keyence VHX-5000 (Keyence Corporation, Osaka, Japan) optical microscope.

We used a glass plate to distribute the glass fibers before producing the microscopic images and examining the fibers. The fibers' length was measured both manually and automatically by optical microscopy. During manual measurement, the length of approximately 1000 randomly selected glass fibers was measured from the materials with each fiber content. In the automatic setting, we did not consider fibers shorter than 0.02 mm and the length of fibers that extended out of the image. For automatic measurements, optical microscopy was combined with image processing software. The computer fitted an ellipse to the fiber, measuring the maximum and minimum diameters. To reduce measurement error, only the ellipse with a D_{max}/D_{min} ratio greater than 5 was considered a fiber, and the length of the major axis of the fitted ellipse approximated its length.

2.2.2. Mechanical tests

Two 5 mm × 80 mm × 1.2 mm rectangular bars per sheet were cut from the injection molded specimens with a cutting disc (Fig. 2) for the mechanical tests. The rectangular bars were cut from the injection-molded specimens using a precision cutting disc to ensure uniform dimensions and minimal thermal or mechanical damage to the material. The cutting process was carefully controlled to avoid introducing additional stresses or defects that could affect the mechanical properties.

The tensile tests and flexural tests were performed on a Zwick Z005 MT (Zwick Roell Group, Ulm, Germany) tester. Before the tests, the specimens were dried at 80 °C for 4 h in Faithful WGLL-125 BE (Faithful Technology, Cangzhou, China) drying oven. During drying, the specimens were stored in a bag containing silica gel to prevent moisture absorption.

The tensile test was performed according to the EN ISO 527-1:2019 standard at a speed of 5 mm/min and a clamping length of 50 mm on 20 dried specimens per test and cycle, but with a specimen geometry different from the standard. We used a 10 kN clamp for the tensile test, and the cross-head movement was used for the evaluation. Tensile strength, Young's modulus, and fracture work were determined from the tensile test. The relationship between mechanical properties and recycling was also investigated with a one-factor analysis of variance (ANOVA). In a one-factor analysis of variance, the mean values of more than two populations are compared according to specified criteria. We examined two cases. First, we compared the average mechanical properties of a material with given fiber content as a function of recycling, and then we compared the average mechanical properties as a function of fiber content when the number of injection molding cycles was the

same.

3. Results and discussion

3.1. Comparing the measurement methods

Our primary goal was to develop an automatic measurement method that makes fast and accurate fiber length measurement possible. For this, we used the automatic setting of the optical microscope software. We measured 1000 of the glass fibers obtained by burning the virgin materials. In order to validate the automatic method, we measured the same number of fibers by hand using the traditional method. In this paper, we compare the two methods. For comparison, we used histograms to calculate the relative density and distribution of fiber length distribution. The relationship between the density function and the distribution function is shown in Eq. (15):

$$f(x) = F'(x) \quad F(x) = \int f(x) dx \quad (15)$$

Selecting the number of bins and resolution is essential when plotting histograms. At few bins, valuable information about the fiber length distribution is lost, while with high resolution, the simple calculation of correlations becomes complicated. Thus, to make the right choice, we examined the changes in numerical and weighted averages for all four materials for different bin numbers. The bins were analyzed on a logarithmic scale in the histogram to emphasize the correlation.

To characterize the fiber length distribution, we used both the average fiber length by Eq. (1) and the fiber length-weighted average by Eq. (16):

$$L_{wk} = \frac{\sum_{i=1}^n w_i^k \cdot N_i \cdot l_i}{\sum_{i=1}^n w_i^k \cdot N_i} \quad (16)$$

where each bin contains N_i fibers of length l_i , and w_i represents the weight based on the fiber length, with $k = 0, \dots, K$ indicating the intensity of the weighting. The weighted average fiber lengths highlight the proportion of longer fibers in the distribution, corresponding to the volume ratio of fibers of different lengths.

We examined the weighted average fiber lengths using different numbers of bins. The results showed that fewer bins led to higher weighted average fiber lengths. To compare the differences across bins, we normalized the average fiber lengths. First, we calculated the average of the weighted fiber lengths for each material. Then, for each group, we divided the average and weighted fiber lengths by that value Eq. (17) and Eq (18):

$$\tilde{L}_N = \frac{L_n}{L_n} = L_n \cdot \frac{n}{\sum_{i=1}^n L_{ni}} \quad (17)$$

$$\tilde{L}_W = \frac{L_{wk}}{L_{wk}} = L_{wk} \cdot \frac{n}{\sum_{i=1}^n L_{wki}} \quad (18)$$

After normalization, it becomes clearer how the averages change as the number of bins increases, and at which point the average values in different bins stop differing significantly. By applying a 5 % error margin to the deviation from the average, we can approximate the minimal number of bins relatively accurately (Fig. 3).

The results indicate that even with ten bins, the average fiber lengths do not differ significantly, but to examine fiber length distribution, we need a sufficient resolution of the data series, for which it is worth using a larger number of bins. In this case, we used 30 bins for the higher resolution of the histogram, with which we get far more accurate results.

The number of histogram bins can generally be determined by taking the square root of the size of the dataset. In this case, the number of bins would be approximately 30, which is a sufficient resolution for examining fiber length distributions and calculating all weighted average fiber lengths. Therefore, we used 30 classes wherever we used

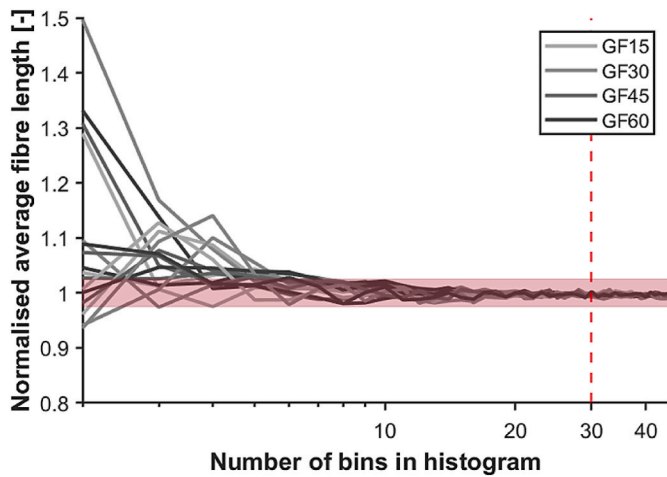


Fig. 3. The deviations of the normalized fiber lengths as a function of bin numbers.

histograms.

3.2. Measurement of fiber length

3.2.1. Fiber length of the initial materials

The effect of fiber shortening during processing was also considered to examine the impact of fiber shortening due to recycling. Therefore, we investigated fiber shortening as a function of both the number of reprocessing cycles and the fiber content of the material. We examined the effect of fiber content on average fiber lengths for the virgin material using both manual and automatic measurements. We fitted an exponential curve on the averages with Eq. (13) (Fig. 4) and found that the linear regression model described our measurement results with sufficient accuracy ($0.8 < R^2 < 1$). With this model Eq. (19), average fiber length can be determined as a function of fiber content within the examined range (15 m%–60 m%).

$$L(X) = a_1 \cdot \exp(-x \cdot a_2) + d, \tag{19}$$

where L is the average fiber length of the given fiber content (X), a_1 and a_2 are constants depending on the material, and d is vertical shift.

The results of both manual and automatic measurements indicate that average fiber length decreased with increasing fiber content. The significant decrease in the averages is presumably caused by fiber breakage during fiber–fiber interaction during the compounding of the material. We compared the weighted averages, and with manual measurement, we did not find a decrease between the averages of 45 m%

and 60 m% glass fiber–reinforced polyamide, while with the automatic method, all average fiber lengths decreased with increasing fiber content. Although the averages are analyzed in the literature with non-weighted and weighted averages, it is worth using stronger weightings because weighting shows better the difference between the averages with increasing fiber content. The advantage of this is, therefore, the increasing sensitivity of measurement. With stronger weighting, the slope increases, emphasizing the difference between the means. Due to the slopes of the curves fitted to the averages, we did not find any significant differences between the two measurement methods, so we examined the fiber length distribution of the reference.

We represented fiber length distribution with the density function belonging to the Weibull distribution, which we fitted to the raw data (Fig. 5). The figures also show the critical fiber length range from the literature (0.18 mm–0.23 mm) for glass fiber–reinforced polyamide (De. et al., 2024).

The results show that there is increasing fiber fragmentation with increasing fiber content. The results obtained from manual measurements showed the expected tendency better, as expected from the literature, i.e., the amount of shorter fibers increased with increasing fiber content. Measurement with the automatic setting showed this tendency to a lesser extent. In all our experiments, we obtained different results with automatic measurement. This is because the automatic image processor cannot account for overlapping fibers, those that hang off the edge of the image, and faintly visible fibers, leading to less reliable results. Additionally, manual adjustments were required to separate and measure the individual fibers. This explains the nature of the histograms and the deviation of the averages from each other. Therefore, in our further tests, we preferred manual measurement.

3.2.2. Fiber length results of recycled materials

We also examined the effect of the number of recycling processes on the average fiber lengths, both for the simple average and the cubic weighted average, using Eq. (20) to fit the curves (Fig. 6):

$$L(n) = a \cdot \exp(-x) + b, \tag{20}$$

where L is the average fiber length after the n th injection molding cycle, a depends on injection molding parameters, and b is the critical fiber length based on the literature (asymptotic limit value).

As the number of recycling cycles increases, average fiber length decreases due to the mechanisms present in processing, which are fiber–melt, fiber–fiber and fiber–machine interactions, and hydrodynamic effects. Based on the percentage difference between the averages, the greatest decrease in fiber length was caused by the second injection molding cycle, except for the 45 m% glass fiber–reinforced polyamide, in which fiber length decreased most during the first injection molding cycle. However, fiber breakage was most significant with increased

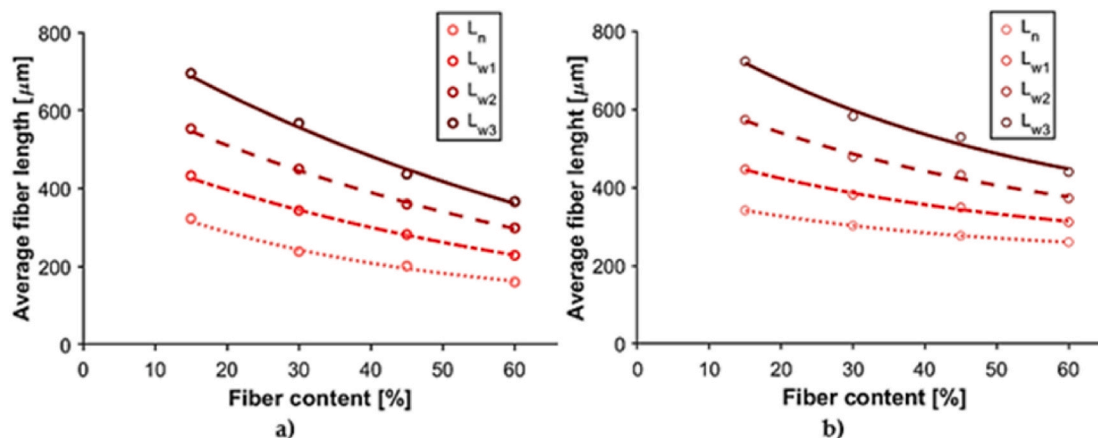


Fig. 4. Average fiber lengths before injection molding as a function of fiber content for a) manual and b) automatic measurement data series.

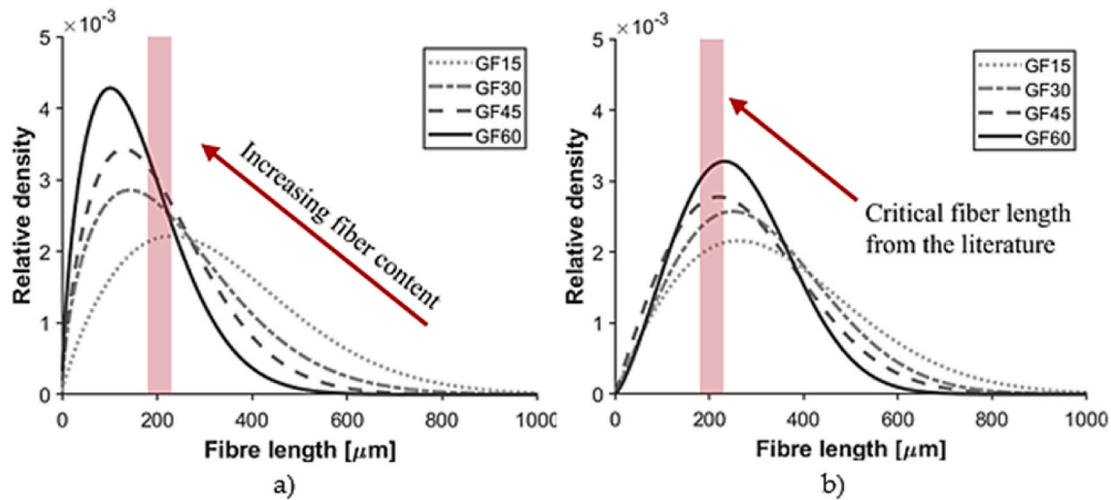


Fig. 5. Fitted Weibull distribution for the polyamide with the four different fiber contents from the data series of a) manual measurement b) automatic measurement.

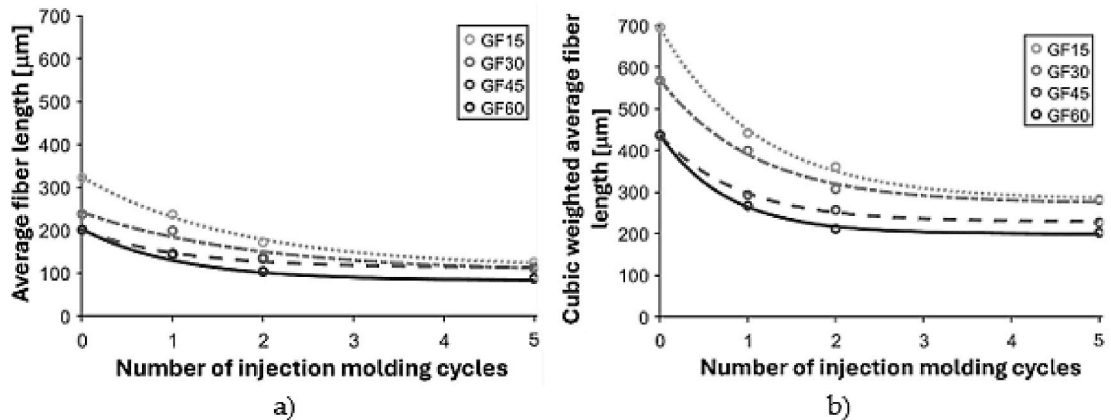


Fig. 6. The effect of recycling on a) average and b) cubic weighted average fiber length (The “0 injection molding cycle” refers to measurements based on pellets.).

weighting during the first injection molding cycle. The fiber shortening that occurs during recycling can be quantified. After the third injection molding, the decrease in average fiber lengths was small, and after the fifth injection molding, it was no longer detectable.

In addition to analyzing the recycling effect, we fitted a Weibull probability distribution to the raw data derived from the fiber length distribution of specimens that had undergone multiple rounds of injection molding (Fig. 7). We used the probability density function of the Weibull distribution in Eq. (3).

The results show that by increasing the number of recycling cycles and fiber content, we get more fibers below the critical fiber length. This significantly affects the load transfer efficiency in the composite, as fibers below the critical fiber length cannot effectively transmit shear loads to the matrix, thereby reducing the overall load-bearing capacity of the material. Consequently, this impacts the mechanical properties of the composite. In addition to the fiber length distribution, we can see an additional relationship if we examine the two parameters of the distribution function: the scale and the shape factor.

For further evaluation we observed the scale and shape parameters of the Weibull distribution function as a function of the effects of fiber content and the number of recycling cycles. According to this, the scale parameter is approximated by an exponential polynomial, as shown below in Eq. (21):

$$s(X_i) = \alpha_1 \cdot \exp(\beta_1 I) + \gamma_1, \tag{21}$$

where $s(X_i)$ is the theoretical scale factor as a function of fiber content

(with 15 m%, 30 m%, 45 m%, and 60 m% glass fiber content), and $\alpha, \beta,$ and γ are technology- and material-dependent parameters. We used a similar relationship for the shape factor's theoretical value, described by Eq. (22).

$$f(X_i) = \alpha_2 \cdot \exp(\beta_2 I) + \gamma_2, \tag{22}$$

where $f(X_i)$ is the shape factor as a function of fiber content. The theoretical factors of the Weibull distribution are shown in Fig. 8.

The scale factors described by the exponential equation are related to the average fiber lengths, which show a decreasing trend as the number of injection molding cycles and the fiber content increase. This trend requires further monitoring because the scale factors probably tend to one point after multiple injection molding cycles due to the high degree of fiber fragmentation. In the shape factor, on the other hand, we experienced a significant difference in the trends between materials with different fiber content.

With the theoretical Weibull parameters, the distribution function for fiber length can be calculated with Eq. (3). The correlation coefficient between the values of the measured and theoretical Weibull fiber length distribution function was $R^2 = 0.981$. The effect of fiber content and recycling on fiber length distribution can be described with high accuracy using Eq. (21) and Eq. (22).

To analyze the mechanical properties, we need to know the percentage of fiber lengths, which provides valuable information about the amounts of fibers that exceed the critical fiber length (Fig. 9). For this, we used the cumulative distribution function (CDF) of the Weibull

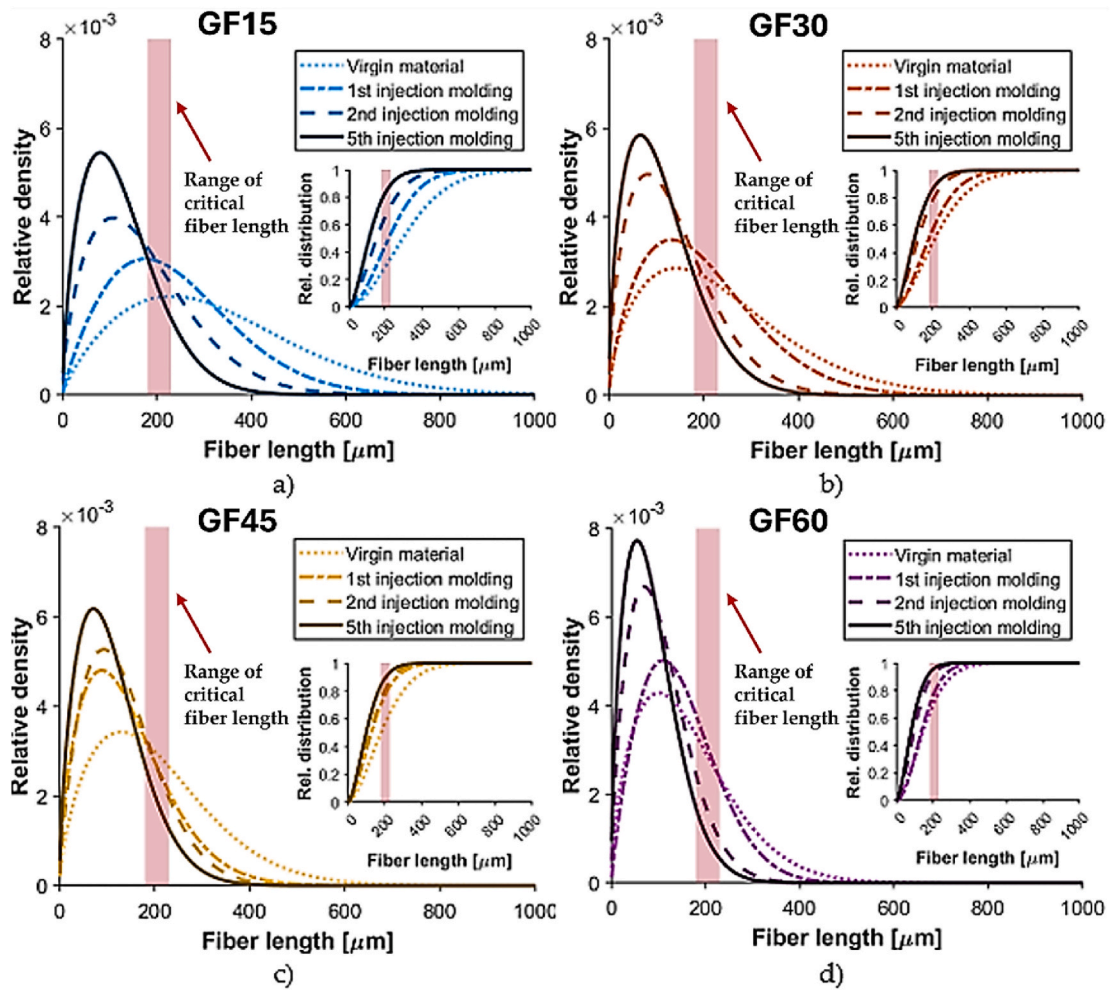


Fig. 7. The effect of the number of injection molding cycles on fiber length distribution, with the critical fiber length range. The Weibull distribution of a) PA6 GF15, b) PA6 GF30, c) PA6 GF 45 and d) PA6 GF60.

distribution Eq. (4).

The percentage of fibers above the critical fiber length (Eq. (23)) can be described from Eq. (4), using the critical fiber length and the Weibull parameters for each material:

$$\lambda_c = p = F(l_c|s, f) = 1 - e^{-\left(\frac{l_c}{s}\right)^f} \quad (23)$$

This allows us to conclude how much fiber fragmentation occurs during injection molding.

3.3. The effect of recycling on mechanical properties

We examined the effect of recycling on mechanical properties obtained from the tensile tests (Fig. 10).

Although increasing the fiber content raised the strength, it also increased the tendency for fiber breakage. The strength increase became progressively smaller as the fiber content increased and decreased after reaching 45 % due to the growing number of fibers below the critical fiber length resulting from fiber-fiber interactions (Fig. 9). In contrast, the modulus increased almost linearly with the fiber content, as it depends on the total fiber volume rather than fiber length (Fig. 10, b). As expected, strain and fracture work decreased exponentially for short-fiber injection-molded composites, but slight variations were observed at lower fiber contents (e.g., GF15), likely due to matrix-dominated behavior and possible molecular degradation effects.

An ANOVA analysis was conducted to evaluate the differences in

mechanical properties across varying fiber contents and recycling cycles. The results showed significant differences in tensile strength as fiber content increased, except between 45 m% and 60 m% for the F2 cycle. Significant differences were observed between the F1 and F2 cycles for most fiber contents, while differences between F2 and F5 cycles were more pronounced for composites with lower fiber contents (e.g., GF15). These findings highlight the combined effects of fiber content and recycling on the mechanical performance of the composites.

The mechanical properties of fiber-reinforced composites are greatly influenced by fiber embedding, which depends on the adhesion at the fiber-matrix interface and the distribution of fiber lengths. Fibers above the critical fiber length contribute significantly to load-bearing capacity, highlighting the importance of investigating how fiber length distributions influence mechanical properties. Fibers above the critical fiber length mainly influenced mechanical properties, so we examined mechanical properties as a function of that (Fig. 11). Fiber content above critical fiber length is given by Eq. (24):

$$\tilde{X} = X \cdot \lambda_c \text{ [m\%]}, \quad (24)$$

where X is fiber content [m%] and λ_c is the percentage of fibers above the critical fiber length [%].

As the number of injection molding cycles increased, the number of fibers below the critical fiber length of the material increased considerably, which led to a decrease in tensile strength (Fig. 11, a). The modulus, however, was independent of the number of fibers above the critical fiber length, as it is primarily influenced by the total fiber volume

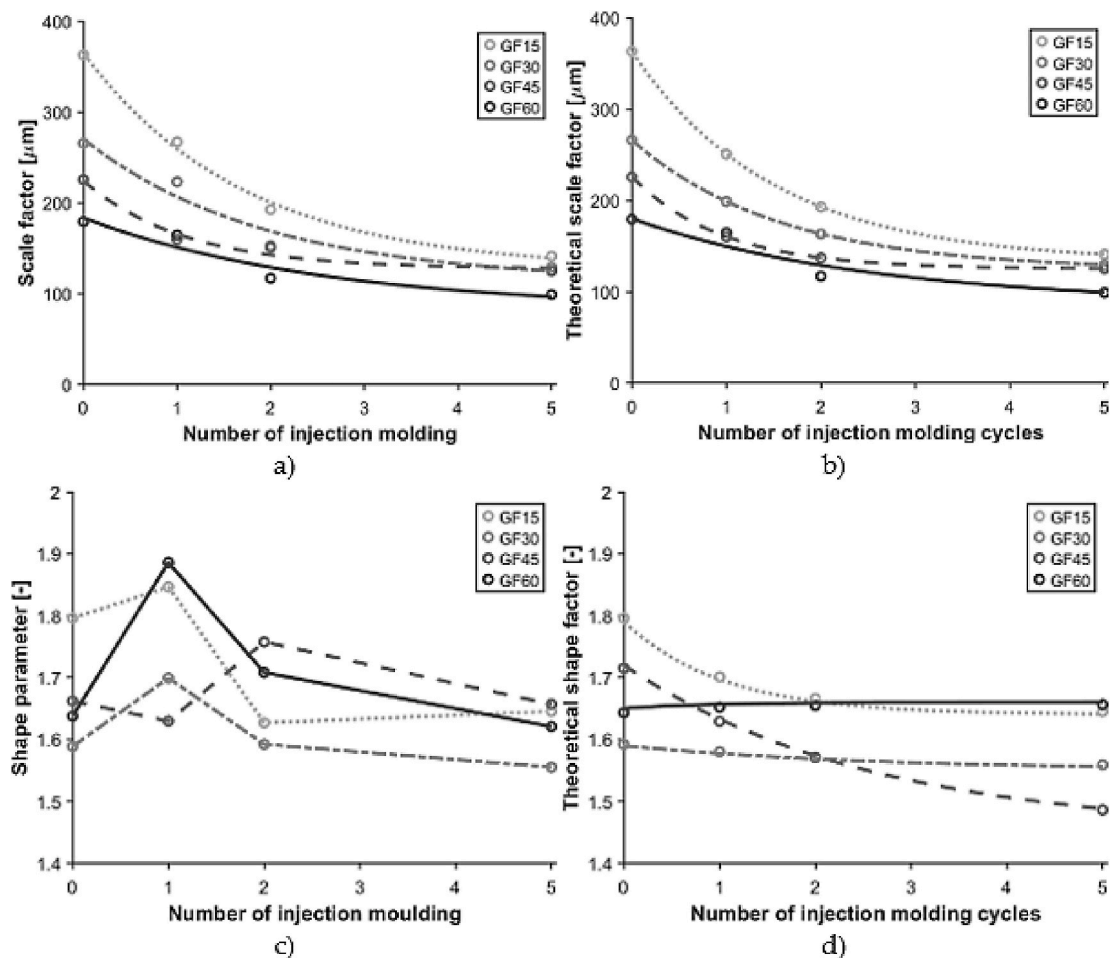


Fig. 8. The actual scale factor (a), theoretical scale factor (b), actual shape factor (c), and theoretical shape factor (d) (The “0 injection molding cycle” refers to measurements based on pellets.).

rather than fiber length and thus was not significantly affected by fiber shortening due to recycling. The tendency of strain and fracture work showed some variation; while both generally decreased with increasing fiber content and recycling cycles, slight increases were observed in lower fiber content samples (e.g., GF15), likely due to matrix-dominated behavior and molecular degradation effects. The results indicate that fiber content had a more significant effect on fiber fragmentation than recycling. The fibers exhibit reduced shear-induced orientation and diminished fiber-fiber interactions during molding at low fiber contents. As a result, despite fiber breakage during multiple recycling cycles, tensile strength remains nearly unchanged while elongation at break increases, indicating enhanced ductility. This can be attributed to the dominant role of the PA6 matrix in load-bearing at low fiber contents. The reduced fiber length decreases stress concentration sites and minimizes microcrack initiation, which would otherwise lead to premature failure. The lower fiber content also allows the matrix to absorb more deformation before failure, resulting in increased elongation. Unlike higher fiber content composites, where fiber breakage significantly compromises mechanical integrity, the ductility of the recycled low-fiber composites is preserved, maintaining their structural performance despite multiple processing cycles. This can be seen in the case of samples containing 15 m% glass fibers (Fig. 11, a).

From the above curves, we extrapolated theoretical curves where all fibers were either above or below the critical fiber length. These theoretical curves can help predict the properties of the injection-molded composite based on whether the fiber lengths are preserved during manufacturing or shortened during processing (Fig. 12).

The calculated theoretical curves (Fig. 12) were created based on the

percentage of fibers above and below the critical fiber length, calculated with Eq. (15). For each fiber content (15 m%, 30 m%, 45 m%, 60 m%), we determined the proportion of fibers above the critical length Eq. (16) and correlated these with the measured tensile strength, modulus, elongation, and fracture work values. Linear fitting equations were applied to these measured properties, and using these equations, we calculated the theoretical values, assuming all fibers were either above or below the critical fiber length. This approach allowed us to define a range for each property at any fiber content, extending from 0 m% (pure PA6 properties) to 60 m% fiber content. The modified rule of mixture from Eq. (21) can be applied to determine the theoretical strength of the composite as a combination of Eq. (6) and Eq. (14).

Due to several factors, very low fiber content can lead to weaker mechanical performance than the pure matrix material. Fibers may be unevenly dispersed at low fiber concentrations and inadequately bonded to the matrix, creating weak points where stress concentrates, leading to premature failure. Instead of reinforcing the material, these weak interfaces can act as spots for crack initiation. Additionally, with fewer fibers, stress may not be distributed uniformly, causing localized stress concentrations and potential crack formation around the fibers, which reduces performance. Non-uniform fiber distribution can also result in regions where the matrix dominates, weakening the material locally and causing failure. Low fiber content reduces toughness, as the remaining fibers may not be sufficient to absorb energy during deformation, leading to brittleness.

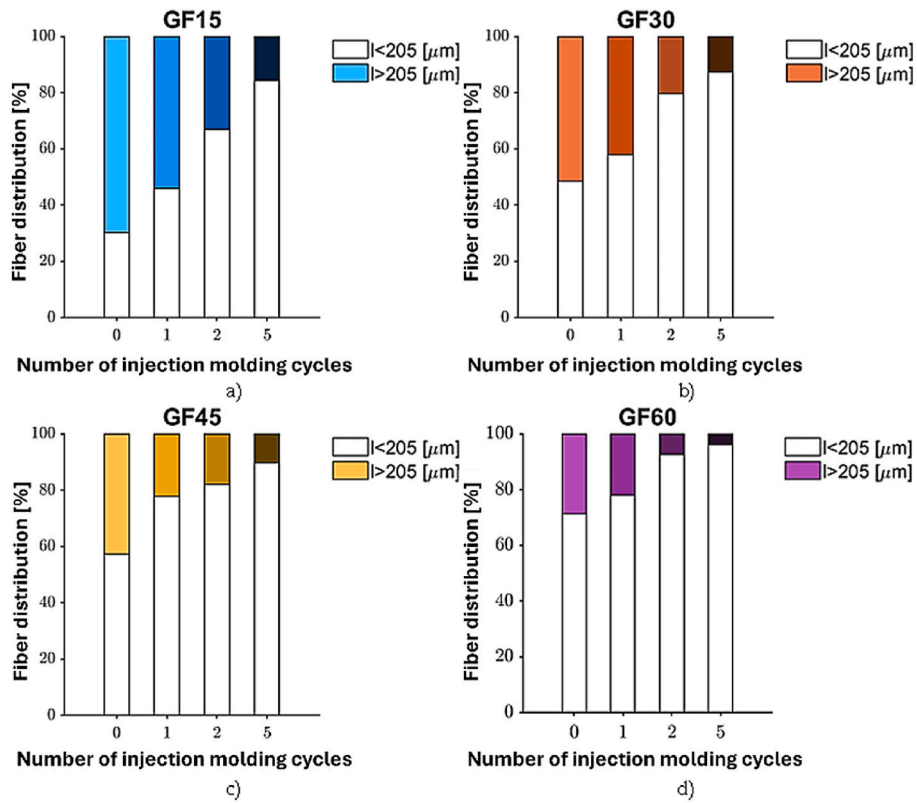


Fig. 9. The effect of recycling on the percentage of fibers under and over the critical fiber length a) PA6 GF15, b) PA6 GF30, c) PA6 GF 45 and d) PA6 GF60 (The “0 injection molding cycle” refers to measurements based on pellets.).

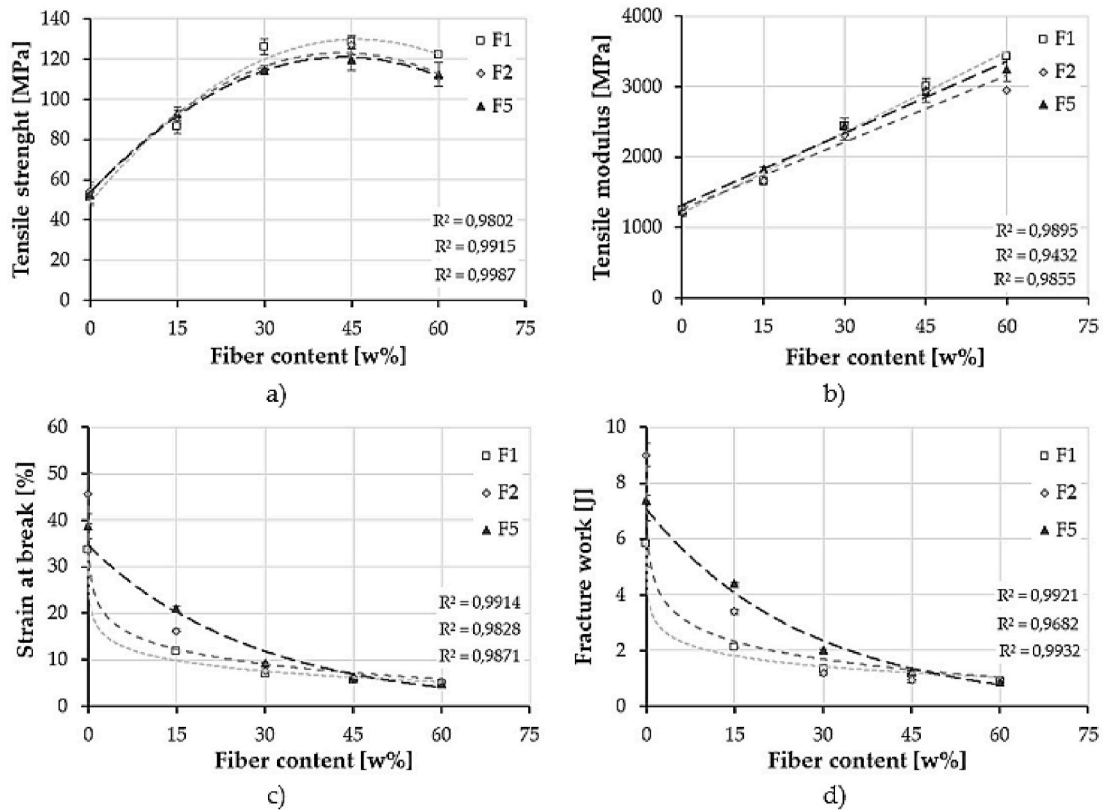


Fig. 10. The effect of recycling on mechanical properties: a) tensile strength, b) modulus of elasticity, c) strain at break, and d) fracture work (F1, F2, and F5 correspond to samples recycled through one, two, and five injection molding cycles, respectively).

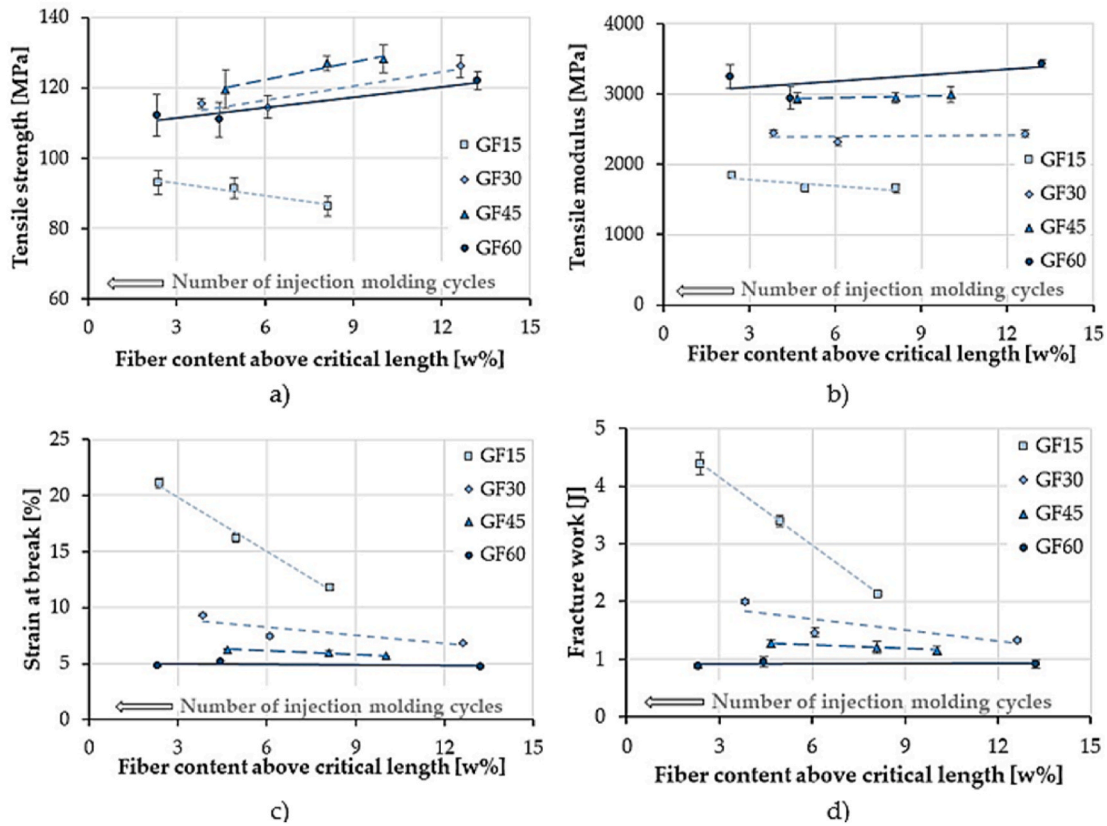


Fig. 11. The effect of fiber content on tensile properties: a) tensile strength, b) modulus of elasticity, c) elongation and d) fracture work.

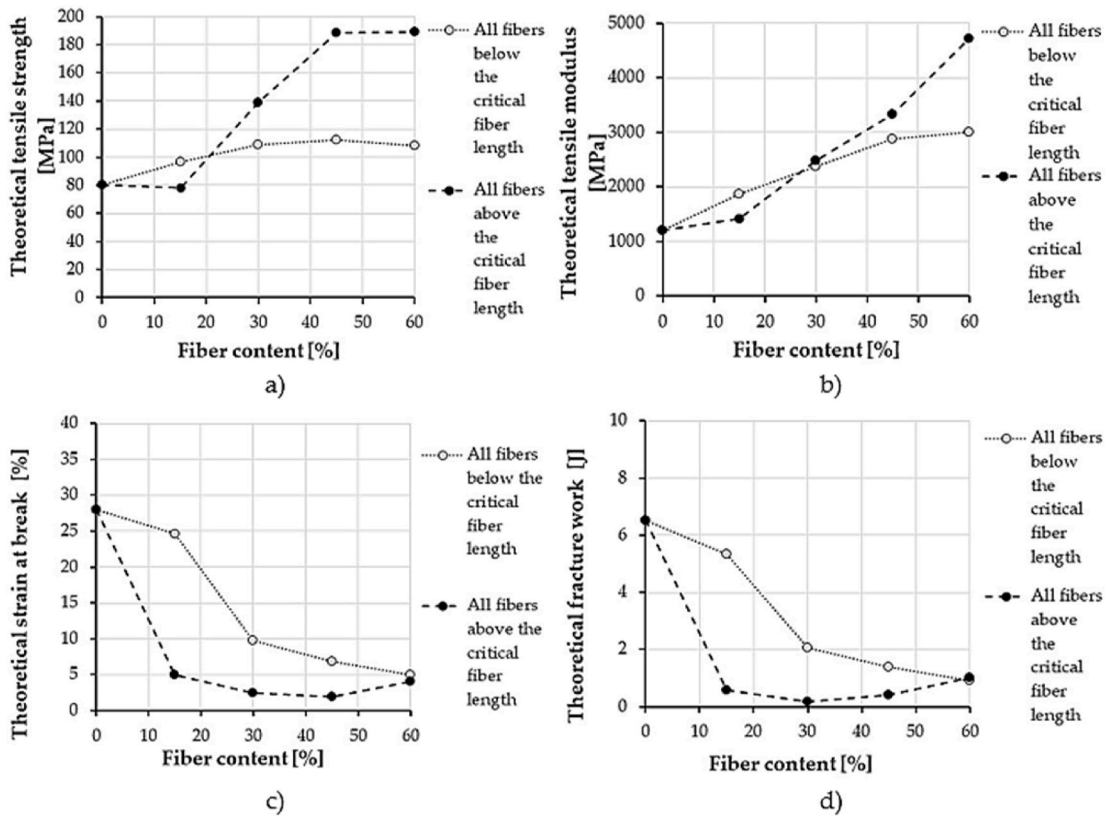


Fig. 12. Calculated theoretical curves based on measurements, assuming that all fibers are either above or below the critical fiber length: a) theoretical tensile strength, b) theoretical modulus of elasticity, c) theoretical elongation at break, and d) theoretical fracture work.

3.4. Effect on carbon footprint

The carbon footprint of materials with varying levels of recycled content (0 %, 15 %, 30 %, 45 %, and 60 %) was evaluated and compared to entirely virgin (neat) materials. Specifically, we calculated the average carbon emissions for injection-molded parts made from polyamide 6 (PA6) reinforced with glass fiber at various percentages (0 %, 15 %, 30 %, 45 %, 60 %) under neat and recycled conditions.

We examined the virgin, one, two, and five times recycled materials in our work. However, in real-world injection molding processes—especially with cold runner systems—recycling occurs by immediately grinding down the runners, which are then directly reintegrated into production. This means that, depending on the level of recycling (Eq. (24)), the material flow will include virgin material, one, two, and, to a lesser extent, multiplied reground material.

$$m_n = x^n(m_0)(1 - x), \quad (24)$$

where m_n is the mass of material ground n times within the product, x is the recycling (regrind) ratio, and m_0 is the product mass.

At typical regrind ratios (10–40 %), with a proportion $(1-x)$ of virgin material, the most significant fraction will consist of material ground once, and a considerable amount of twice-ground material will appear. Materials ground more than five times will be present in only negligible quantities. This is why we performed measurements in earlier experiments with materials that had been entirely reground once, twice, or five times, as the above equation allows for calculating the composite properties for any recycling ratios.

This calculation also applies to carbon footprint, with the difference being that only the carbon footprint of the injection molding machine, temperature controller, and feeders must be considered for virgin material. In cases involving recycled material, the carbon footprint of the grinder also enters the calculation, though there is no need to account for the carbon footprint of raw material production for the recycled portion. We used guideline values from raw material and equipment manufacturers for these calculations.

The initial results (Fig. 13) provide the average emissions (kg CO₂ per kg of PA6) associated with each material configuration. As anticipated, higher recycled content led to a reduction in carbon footprint across all levels of glass fiber reinforcement, with a progressive decrease in emissions as the proportion of recycled material increased. This observation aligns with findings from previous studies on glass fiber-reinforced composites, which emphasize the environmental benefits of using recycled materials in polymer matrices.

Following this, we normalized the carbon footprint per unit of mechanical strength (g CO₂/kg PA6/MPa) to evaluate the emissions relative to the material's mechanical performance (Fig. 14). This analysis reveals that increasing the glass fiber content enhances strength and significantly raises emissions. As a result, configurations with higher

reinforcement levels do not necessarily offer the best environmental outcomes when balancing strength and sustainability. The findings are consistent with recent studies suggesting that the degradation of mechanical properties in recycled polymers, such as fiber length reduction and matrix viscosity changes, can impact the material's strength-to-emission ratio.

The data indicate that the highest glass fiber content does not yield the optimal balance between mechanical performance and carbon footprint. Instead, a moderate level of reinforcement (30 %, 45 %) combined with recycled content provides a more sustainable option, supporting structural integrity while minimizing environmental impact. This optimal configuration reflects a growing interest in achieving a circular economy in polymer manufacturing, where resource efficiency is maximized without compromising product durability.

4. Conclusion

The findings of this study demonstrate that recycled glass fiber-reinforced polyamide composites retain adequate mechanical properties for certain applications, even as fiber length and performance degrade across recycling cycles. By examining the effects of glass fiber content (15 %, 30 %, 45 %, and 60 %) and recycling cycles, we found that fiber fragmentation increases with each cycle, reducing average fiber length and negatively impacting tensile strength and modulus. Notably, while higher fiber content initially enhances performance, it declines beyond 45 % due to excessive fiber-fiber interaction-induced breakage.

Using a Weibull probability distribution model, we characterized fiber length distribution and found that recycling increases the proportion of shorter fibers, which reduces tensile strength. However, the elastic modulus remained stable, as it depends on total fiber volume rather than fiber length. Low fiber content introduced weak points, reducing toughness and mechanical integrity, sometimes performing worse than the pure matrix material.

The approach presented in this study applies to a wide range of fiber-reinforced composite systems, particularly those involving short or chopped fibers such as glass, carbon, or natural fibers embedded in thermoplastic matrices. The methodology for evaluating fiber length distribution, mechanical performance, carbon footprint, and recycling effects can be extended to other polymeric systems where fiber fragmentation and its impact on mechanical integrity are of concern. Additionally, the statistical methods used in this study, including analysis of variance (ANOVA) and fiber length distribution modeling, can be adapted to analyze similar degradation and performance trends in other composite materials.

However, it is essential to acknowledge certain limitations. The findings and interpretations are specific to the studied polyamide-based composites with glass fiber reinforcement and may not fully capture the complexities of other material systems, such as those with different fiber-matrix interactions, processing conditions, or recycling methods. Furthermore, while the statistical approaches provide meaningful insights into fiber degradation trends, they may require adaptation or additional validation when applied to materials with significantly different mechanical behaviors or failure mechanisms.

In conclusion, optimizing fiber content and recycling practices is critical to ensuring the long-term durability and reliability of recycled composites. Moderate reinforcement levels combined with recycled content provide an optimal balance between mechanical performance and environmental impact, supporting their use in automotive applications. This highlights the importance of effective recycling process control and composite design in transitioning toward a circular economy in the automotive industry.

CRedit authorship contribution statement

Maja Csapó: Writing – original draft, Investigation, Formal analysis,

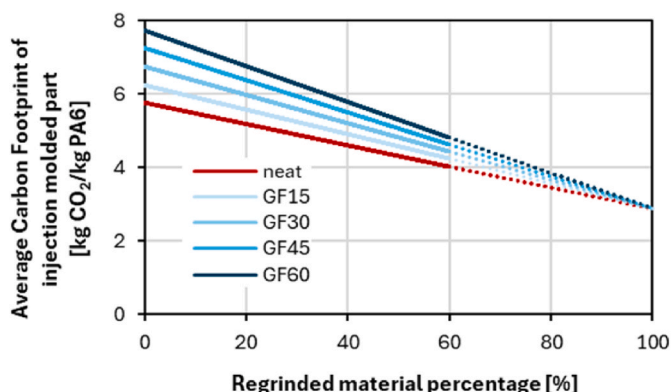


Fig. 13. Average Carbon Footprint of injection molded part (kg CO₂/kg PA6).

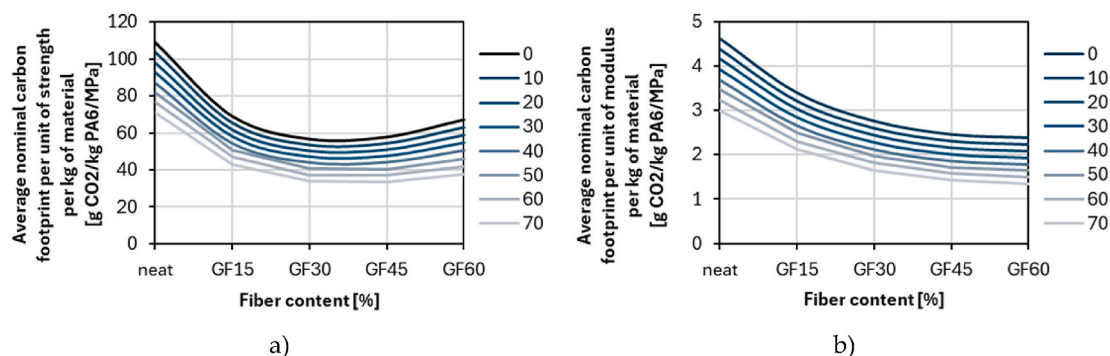


Fig. 14. Average nominal carbon footprint per unit of mechanical performance per kg of material (g CO₂/kg PA6/MPa): (a) strength, (b) modulus.

Data curation. **József Gábor Kovács**: Writing – review & editing, Writing – original draft, Validation, Supervision, Resources, Project administration, Methodology, Investigation, Funding acquisition, Formal analysis, Conceptualization.

Funding

This work was supported by the National Research, Development and Innovation Office, Hungary (2020-1.2.3-EUREKA-2021-00010, 2023-1.1.1-PIACI_FÓKUSZ-2024-00011). This research was funded by the Horizon Europe Framework Programme and the call HORIZON-WIDERA-2021-ACCESS-03, under the grant agreement for project 101 079 051 – IPPT_TWINN. The research was done under the scope of the Project no. RRF-2.3.1-21-2022-00009, entitled “National Laboratory for Renewable Energy” which has been implemented with the support provided by the Recovery and Resilience Facility of the European Union within the framework of Programme Széchenyi Plan Plus. Project no. TKP-6-6/PALY-2021 has been implemented with the support provided by the Ministry of Culture and Innovation of Hungary from the National Research, Development and Innovation Fund, financed under the TKP2021-NVA funding scheme. The project supported by the Doctoral Excellence Fellowship Programme (DCEP) is funded by the National Research Development and Innovation Fund of the Ministry of Culture and Innovation and the Budapest University of Technology and Economics.

Declaration of competing interest

The authors declare that they have no known competing financial interests or personal relationships that could have appeared to influence the work reported in this paper.

Acknowledgment

We wish to thank Arburg Hungária Kft. for the ARBURG Allrounder 470 A 1000-290 injection molding machine, Tool-Temp Hungária Kft., Lenzkes GmbH, and Piovan Hungary Kft. for the accessories. Additionally, we extend our gratitude to Grupa Azoty S.A., Tarnów, Poland, for providing all the Tarnamid materials.

Data availability

Data will be made available on request.

References

Bernasconi, A., Rossin, D., Armani, C., 2007. Analysis of the effect of mechanical recycling upon tensile strength of a short glass fiber reinforced polyamide 6,6. *Eng. Fract. Mech.* 627–641.

Bernasconi, A., Davoli, P., Rossin, D., Armani, C., 2007. Effect of reprocessing on the fatigue strength of a fibreglass reinforced polyamide. *Composites Part A* 38, 710–718.

Breuer, K., Spickehuer, A., Stommel, M., 2021. Statistical analysis of mechanical stressing in short fiber reinforced composites by means of statistical and representative volume elements. *Fibers* 9 (32).

Cai, H., Je, J., Wang, Y., Saafi, M., Ye, J., 2023. Microscopic failure characteristics and critical length of short glass fiber reinforced composites. *Composites, Part B* 266, 110973.

Curtis, P.T., Bader, M.G., Bailey, J.E., 1978. The stiffness and strength of a polyamide thermoplastic reinforced with glass and carbon fibres, 13 (2), 377–390.

De, B., Bera, M., Bhattacharjee, D., Ray, B.C., Mukherjee, S., 2024. A comprehensive review on fiber-reinforced polymer composites: raw materials to applications, recycling, and waste management. *Prog. Mater. Sci.* 146.

Ding, J., Chen, G., Huang, W., Cheng, J., Li, T., Cheng, C., Xu, J., 2024. Tensile strength statistics and fracture mechanism of ultra high molecular weight polyethylene fibers: on the weibull distribution. *ACS Omega* 9, 12984–12991.

Dollischek, L.B., Frohn-Sörensen, P., Kurz, F., Engel, B., 2024. Injection molding of post-industrial recycled glass fiber reinforced polyphenylene sulfide (PPS GF40): industrial feasibility and material analysis. *J. Clean. Prod.* 471, 143416.

Eriksson, P.-A., Albertsson, A.-C., Boydell, P., Eriksson, K., Manson, J.-A.E., 1996. Prediction of mechanical properties of recycled fibreglass reinforced polyamide 66. *Polym. Compos.* 17 (6), 830–839.

Giusti, R., Zanini, F., Lucchetta, G., 2018. Automatic glass fiber measurement for discontinuous fiber-reinforced composites. *Composite Science Part A* 112, 263–270.

Goncalves, R.M., Martinho, A., Oliveira, J.P., 2022. Recycling of reinforced glass fibers waste: current status. *Materials*.

Gopalraj, S.K., Karki, T., 2020. A Review on the Recycling of Waste Carbon fibre/glass fiber-reinforced Composites: Fibre Recovery, Properties and Life Cycle Analysis. *SN Applied Science*.

Güllü, A., Özdemir, A., Özdemir, E., 2006. Experimental investigation of the effect of glass fibres on the mechanical properties of polypropylene (PP) and polyamide 6 (PA6) plastic. *Mater. Des.* 27, 316–323.

Inoue, A., Morita, K., Sawada, Y., 2015. Effect of screw design on fiber breakage and dispersion in injection-molded long glass-fiber-reinforced polypropylene. *J. Compos. Mater.* 49 (1).

Kang, D., Lee, J.M., Moon, C., Kim, H.-I., 2021. Improvement in mechanical properties of recycled polypropylene composite by controlling the length distribution of glass-fibers. *Polym. Compos.* 42, 2171–2179.

Kang, B., Kim, D., Sohn, J.S., Park, N., Kim, K., Kim, H.J., Koh, Y., Choi, B.H., 2024. Observations of Short- and long-term mechanical properties of glass fiber reinforced polypropylenes with post-consumer recycled materials. *International Journal of Precision Engineering and Manufacturing-Green Technology* 11, 523–535.

Karimi, S.M., Neitzel, B., Lang, M., Puch, Florian, 2023. Investigation of the fiber length and the mechanical properties of waste recycled from continuous glass fiber-reinforced polypropylene. *Recycling* 8, 82.

Kugler, S.K., Kech, A., Cruz, C., Osswald, T., 2020. Fiber orientation predictions a review of existing models. *Journal of Composites Science* 4, 69.

Kuram, E., Tasci, E., Altan, A.I., Medar, M.M., Yilmaz, F., Ozcelik, B., 2013. Investigating the effects of recycling number and injection parameters on the mechanical properties of glass-fibre reinforced nylon 6 using taguchi method. *Mater. Des.* 49, 139–150.

Lafranche, E., Krawczak, P., Ciolczyk, J., Maugey, J., 2005. Injection moulding of long glass fibre reinforced polyamide 66: processing Conditions/microstructure/Flexural properties relationship. *Adv. Polym. Technol.* 24 (2), 114–134.

Miscik, S., Dobránsky, J., Gombár, M., Cep, R., 2024. Determination of the brittleness of glass fibers on selected mechanical and rheological properties of the polymer composite. *Express Polym. Lett.* 18 (No.10), 1051–1062.

Moussaoui, H., 2024. Achieving energy savings and process optimization in plastic injection molding: a design of experiments study. *J. Clean. Prod.* 477, 143835.

Nguyen, D.T., Yu, E., Barry, C., Chen, W.-T., 2024. Energy consumption variability in life cycle assessments of injection molding processes: a critical review and future outlooks. *J. Clean. Prod.* 452, 142229.

Pietroluongo, M., Padovano, E., Frache, A., Badini, C., 2020. Mechanical recycling of an end-life-automotive composite component. *Sustain. Mater. Technol.*

Rohde, M., 2015. Direct Processing of Long Fiber Reinforced Thermoplastics Composites and their Mechanical Behaviour Under Static and Dynamics Load. University of Bayreuth Thesis.

- Salaberger, D., Kannappan, K.A., Kastner, J., Reussner, J., Auinger, T., 2011. Evaluation of computed tomography data from fibre reinforced polymers to determine fibre length distribution. *Int. Polym. Process.* 26 (3), 283–291.
- Tamrakar, S., Couvreur, R., Mielewski Jr., D., Gillespie, W.J., 2023. Effects of recycling and hygrothermal environment on mechanical properties of thermoplastic composites. *Polym. Degrad. Stabil.* 207.
- Tinz, J., de Ancos, T., Volker, F., Rohn, H., 2023. Application of allocation methods in open-loop recycling systems: the carbon footprint of injection molded products based on ABS, PA66GF30, PC and POM. *Resources, Conservation & Recycling Advances* 19, 200176.
- Turkovich, V.R., Erwin, L., 1983. Fiber fracture in reinforced thermoplastics processing. *Polym. Eng. Sci.* 23 (13), 743–749.
- Vas, L.M., 2006. Strength of unidirectional short fiber structures as a function of fiber length. *J. Compos. Mater.* 40 (19), 1695–1734.